Coupled Parity-Time Symmetric Cavities: Results from Transmission Line Modelling Simulations

Sendy Phang[1], Ana Vukovic[1], Stephen C. Creagh[2], Gabriele Gradoni[2], Phillip D. Sewell[1], Trevor M. Benson[1]

[1] *George Green Institute for Electromagnetics Research, University of Nottingham, University Park, Nottingham, NG7 2RD, UK*

[2] *School of Mathematical Sciences, University of Nottingham, University Park, Nottingham, NG7 2RD, UK*

e-mail: sendy.phang@nottingham.ac.uk

ABSTRACT

This paper studies the impact of a dispersive gain/loss material model on Parity-Time (PT) coupled microresonator cavity structures using the time-domain Transmission-Line Modelling method. A modal analysis is also performed to compare the modal composition in the dispersive and non-dispersive cases. Furthermore, a waveguide-to-waveguide coupler based on the coupled PT-resonant microresonators is analysed to see how the resulting modal profiles are manifested in the power transmitted between input/output ports.

Keywords: parity-time, coupled microcavities, amplifier and coupler, Transmission Line Modelling (TLM) method.

1. INTRODUCTION

Photonic structures with balanced gain and loss that mimic the parity-time (PT) symmetric Hamiltonians in quantum field theory have been a subject of intense investigation due to their unique properties [1,2]. PT symmetric structures in photonics are constructed by requiring that the material refractive index profile satisfies $n(\boldsymbol{r}) = n^*(-\boldsymbol{r})$ where $\boldsymbol{r}$ denotes the position and $*$ denotes complex conjugate operator. In such a configuration, the real part of the refractive index is an even function whilst the imaginary part of the refractive index is an odd function of space. This condition requires the structure to be comprised of equal amounts of gain and loss. The main feature of PT-symmetric structures is the existence of a threshold point that describes the amount of modal gain and loss in the system. If the system has gain/loss below the threshold point the eigenvalues are real, whilst above the threshold point the eigenvalues form a complex conjugate pair [1,3–6]. PT-symmetric photonic structures based on Bragg gratings, coupler waveguides, lattices and resonant cavities have been studied theoretically and experimentally and shown to exhibit directionally dependent properties, such as loss-induced unidirectional invisibility, simultaneous laser and coherent absorber modes and loss-induced lasing. A range of applications such as switching, logical-gate operation, laser and memory have been proposed based on the existence of the threshold and their directional dependent property [7–14].

In this paper the eigenfrequencies of an isolated coupled PT-microcavity are analysed under the condition that the material is dispersive and that gain/loss model satisfies the Kramers-Kronig relations. The modelling is done using the numerical time-domain Transmission-Line Modelling (TLM) method. Furthermore, the analysis is extended to a practical scenario where PT-microcavities are used to couple energy between input/output waveguide channels.

2. PARITY-TIME (PT) SYMMETRIC COUPLED CAVITIES

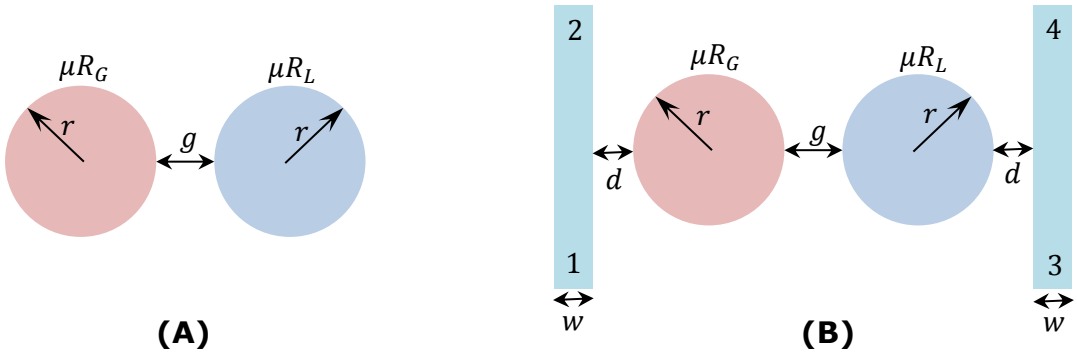

Figure 1(A) Isolated PT-coupled resonant cavities and (B) PT-resonant coupler where PT-coupled resonant cavities are placed between the input and output waveguides.

Two configurations of PT-coupled resonant cavities that are investigated in this paper are shown in Fig. 1. The isolated PT-resonant cavities are shown in Fig. 1(A). Microresonators μR_G and μR_L denote the gain and lossy resonator respectively. Both resonators have the same radius r and are separated by a gap g. Figure 1(B) shows the coupled PT-microresonators placed between two passive waveguides with a waveguide to resonator separation of d. The waveguides have the same width w and refractive index n and the ports are denoted as 1-4. The background in both Figs. 1(A, B) is considered to be air.

To model these structures, a time-domain numerical model namely the transmission-line modelling (TLM) method is used [15,16]. The TLM method is based on the analogy between the propagating electromagnetic fields and voltage impulses traveling on an interconnected mesh of transmission lines (TL). Successive repetitions of a scatter–propagate procedure provide an explicit and stable time stepping algorithm that mimics electromagnetic field behaviour to second-order accuracy in both time and space [15,16]. In this paper for the two-dimensional problem in Fig. 1 E-polarised waves are considered. The Lorentzian model for material properties is used to describe dispersive gain/loss model that satisfies the Kramers-Kronig relations as [17,18],

$$\varepsilon(\omega) = \varepsilon_\infty - j\frac{\sigma_0}{2\omega\varepsilon_0}\left[\frac{1}{1+j(\omega-\omega_\sigma)\tau} + \frac{1}{1+j(\omega+\omega_\sigma)\tau}\right], \tag{1}$$

where ε_∞ denotes the dielectric constant at infinity, ω_σ denotes the atomic transitional angular frequency, τ is the atomic relaxation time parameter and σ_0 denotes the peak conductivity that is set by the pumping level at ω_σ. The time dependent field component has been assumed in the form of $\exp(j\omega t)$, so that $\sigma_0 > 0$ denotes loss while $\sigma_0 < 0$ denotes gain. The frequency dependent complex refractive index is expressed as $\sqrt{\varepsilon(\omega)}$ and the gain-loss parameter is defined by the imaginary part of the refractive index as $\alpha = \omega n''$. The implementation of the dispersive gain/loss model in the TLM is done using the bilinear-transformation technique, as described in [16], and has also previously been used to model PT-Bragg gratings as in [13].

3. MODAL ANALYSIS OF PT-COUPLED RESONANT CAVITIES

In this section, the modal composition of the isolated PT-coupled resonant cavities depicted in Fig. 1(A) with a dielectric constant of $\varepsilon_\infty = 12.25$ and an air ($n = 1$) background material is considered. The coupled resonators have a radius $r = 0.54$ µm and are separated by $g = 0.15$µm. The cavities are operated at a high Q-factor mode of (10,1) where (m,n) denotes the azimuthal and radial mode order respectively. The resonant frequency of the high Q-factor mode is $f_0^{(10,1)} = 336.81$ THz with the Q-factor $Q = 1.05 \times 10^7$. The structure is discretised using a uniform square mesh of size $\Delta x = 2.5$ nm. The excitation is a Gaussian dipole with a FWHM of 250 fs modulated at $f_0^{(10,1)}$ inside the gain resonator and the simulation is run for total time of 2.3ps. A set of time-domain simulation data is recorded by a point monitor located in the lossy resonator. Discrete spectra are obtained from the time-domain simulation data by using the "Harminv" program, an implementation of the filter diagonalization method [19] available at [20].

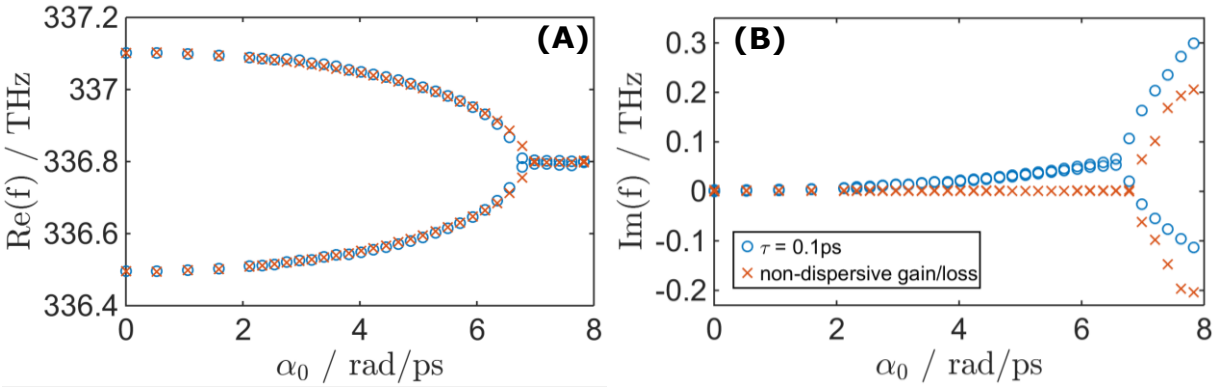

Figure 2(A) the real part and (B) the imaginary part of the eigenfrequencies of the isolated PT-coupled resonant cavities as a function of gain/loss parameter $\alpha_0 = \omega_0 n''$.

Figure 2 depicts the eigenfrequencies of the isolated PT-coupled resonant cavities as a function of gain-loss parameter $\alpha_0 = \omega_0 n''$ for both dispersive and non-dispersive gain/loss material models. The gain and loss is assumed to be tuned at the resonant frequency of a single resonator, i.e. $\omega_\sigma = 2\pi f_0^{(10,1)}$ with the atomic

relaxation time of $\tau = 0.1$ps. Figure 2(A) shows that the real parts of the eigenfrequencies are beating, are centred at $f_0^{(10,1)}$, and coalesce at the threshold point. After the threshold point, the real part of the eigenfrequency is no longer beating but remains constant at $f_0^{(10,1)}$. Note that the agreement is very good between the PT resonators with dispersive and ideal gain/loss material model both before and after the threshold, with only minor discrepancies around the threshold point. The imaginary parts of the eigenfrequenices for the cases of the dispersive and non-dispersive gain/loss material models are plotted in Fig. 2(B) for different gain/loss parameters. It can be seen that in the absence of gain/loss, $\alpha_0 = 0$, the imaginary parts of the eigenfrequencies are almost zero, as the high Q-factor implies a low radiation loss. For the case of the non-dispersive gain/loss model, the imaginary parts of the eigenfrequencies remain constant at $\mathrm{Im}(f) \approx 0$, and split at the threshold point forming a complex conjugate pair. Meanwhile for the case of the dispersive gain/loss model, as the gain/loss parameter increases the imaginary part of the eigenfrequencies increases, i.e., the eigenvalues are becoming more lossy below the threshold point. At the threshold point the imaginary part splits asymmetrically meaning that above the threshold, and in the presence of dispersion, eigenvalues are not a complex conjugate pair. Similar modal behaviour was also noted in a recent publication [18] in which the resonant frequencies of the coupled PT-microcavities were calculated analytically by solving Green's integral equation.

4. PT-RESONANT DIRECTIONAL COUPLER

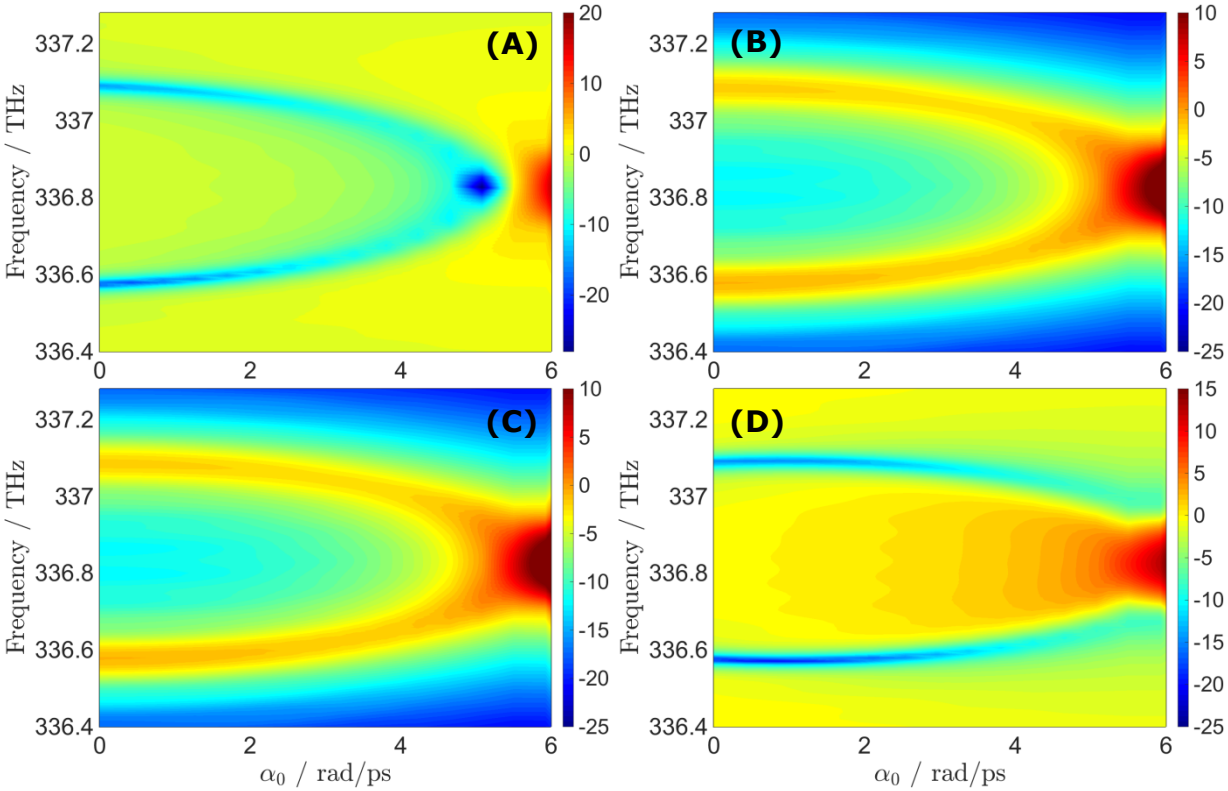

Figure 3. Transmittance of PT-coupled resonant cavities as an optical circuit component. (A) the bar transmittance T_{12}; (B) the cross transmittance T_{14} when port 1 is excited; (C) the cross transmittance T_{41}; (D) the bar transmittance T_{43} when port 4 is excited;

This section investigates the real-time behaviour of the PT-microresonators in the context of the coupler. The coupled PT-resonators have the radius $r = 0.54$µm and are separated by a gap $g = 0.16$µm. Two passive waveguides of width $w = 0.15$µm, separated by $d = 0.16$µm from a resonator and having a refractive index $n = 3.5$ are introduced as a way of coupling input signal to cavities. Two different excitations ports are considered, i.e. port 1 and port 4. In both cases, the waveguide is operated as a single mode at $f_0^{(10,1)}$ with a modal effective index of $n_{eff} = 2.966$. In the case of port 1 excitation, two different transmissions occur,

namely direct transmission T_{12} and cross transmission T_{14}. On the other hand, if port 4 is excited, the direct transmission is T_{43} and the cross transmission is T_{41}.

The direct transmittance for port 1 excitation, T_{12} is displayed in Fig. 3(A) in a log scale as a function of gain/loss parameter α_0. Figure 3(A) shows very low T_{12}transmittance at the frequencies corresponding to the beating frequencies of the coupled PT-resonant cavities. As the gain/loss parameter increases this minimum transmittance coalesce at the threshold point creating a no transmission point at the $f_0^{(10,1)}$. The cross transmittance T_{14} depicted in Fig 3(B), shows that in the absence of gain/loss $\alpha_0 = 0$, the transmitted spectra are related to the beating frequencies between the resonators. As the gain/loss increases this transmitted signal coalesces at the threshold point. A further increase in the gain/loss parameter causes lasing to occur at ports 2 and 4.

Figures 3(C,D) show the case when port 4 is excited, with the cross transmittance T_{41} shown in Fig.3(C) and the direct transmittance T_{43} shown in Fig.3(D). In the case of cross transmittance T_{41} only the spectra related to the beating frequencies are transmitted across from port 4 to port 1. As the gain/loss increases these transmitted spectra coalesce at the threshold point and lasing is observed above the threshold point. The direct transmittance of T_{43} depicted in Fig. 3(D) shows that in the absence of gain/loss $\alpha_0 = 0$, there is no transmission on the two frequencies related to the beating frequencies of the coupled resonators. Further increase of gain/loss causes an amplification of transmission of signal frequencies in the range between these two frequencies. It is important to note the fact that $T_{14} = T_{41}$, i.e. that Lorentz reciprocity [21] is preserved in PT-coupled resonators.

5. CONCLUSION

In this paper, we show that PT-coupled resonant cavities with a dispersive material gain/loss model preserves the threshold point found in ideal non-dispersive PT resonant structures. However, it is found that in the case of dispersive materials the eigenfrequencies are not a complex conjugate pair but are skewed more towards the lossy mode. Furthermore, the transmission response of the PT resonant directional coupler is analysed for different amounts of gain/loss in the model. It is shown that, depending on the direction of excitation, the coupler exhibits an asymmetric response in bar transmission whilst the cross transmission is preserved.

6. REFERENCES

1. Y. D. Chong, L. Ge, and A. D. Stone, "PT-Symmetry Breaking and Laser-Absorber Modes in Optical Scattering Systems," Phys. Rev. Lett. 106, 093902 (2011).
2. C. M. Bender, S. Boettcher, and P. N. Meisinger, "PT-symmetric quantum mechanics," J. Math. Phys. 40, 2201 (1999).
3. H. Benisty, C. Yan, A. Degiron, and A. Lupu, "Healing Near-PT-Symmetric Structures to Restore Their Characteristic Singularities: Analysis and Examples," J. Light. Technol. 30, 2675–2683 (2012).
4. S. Longhi, "Optical Realization of Relativistic Non-Hermitian Quantum Mechanics," Phys. Rev. Lett. 105, 013903 (2010).
5. C. E. Rüter, K. G. Makris, R. El-Ganainy, D. N. Christodoulides, M. Segev, and D. Kip, "Observation of parity–time symmetry in optics," Nat. Phys. 6, 192–195 (2010).
6. J. Čtyroký, V. Kuzmiak, and S. Eyderman, "Waveguide structures with antisymmetric gain/loss profile," Opt. Express 18, 21585–21593 (2010).
7. F. Nazari, M. Nazari, and M. K. Moravvej-Farshi, "A 2×2 spatial optical switch based on PT-symmetry.," Opt. Lett. 36, 4368–70 (2011).
8. A. Lupu, H. Benisty, and A. Degiron, "Switching using PT symmetry in plasmonic systems: positive role of the losses," Opt. Express 21, 192–195 (2013).
9. S. Phang, A. Vukovic, H. Susanto, T. M. Benson, and P. Sewell, "Ultrafast optical switching using parity–time symmetric Bragg gratings," J. Opt. Soc. Am. B 30, 2984–2991 (2013).
10. M. Kulishov, B. Kress, and R. Slavík, "Resonant cavities based on Parity-Time-symmetric diffractive gratings," Opt. Express 21, 68–70 (2013).
11. B. Peng, . K. Ozdemir, S. Rotter, H. Yilmaz, M. Liertzer, F. Monifi, C. M. Bender, F. Nori, and L. Yang, "Loss-induced suppression and revival of lasing," Science (80-.). 346, 328–32 (2014).

12. X. Zhu, L. Feng, P. Zhang, X. Yin, and X. Zhang, "One-way invisible cloak using parity-time symmetric transformation optics.," Opt. Lett. 38, 2821–4 (2013).
13. S. Phang, A. Vukovic, H. Susanto, T. M. Benson, and P. Sewell, "Impact of dispersive and saturable gain/loss on bistability of nonlinear parity-time Bragg gratings.," Opt. Lett. 39, 2603–6 (2014).
14. S. Phang, A. Vukovic, T. M. Benson, H. Susanto, and P. Sewell, "A versatile all-optical parity-time signal processing device using a Bragg grating induced using positive and negative Kerr-nonlinearity," Opt. Quantum Electron. 47, 37–47 (2015).
15. C. Christopoulos, The Transmission-Line Modeling Method TLM (IEEE Press, 1995).
16. J. Paul, C. Christopoulos, and D. W. P. Thomas, "Generalized material models in TLM .I. Materials with frequency-dependent properties," IEEE Trans. Antennas Propag. 47, 1528–1534 (1999).
17. S. C. Hagness, R. M. Joseph, and A. Taflove, "Subpicosecond electrodynamics of distributed Bragg reflector microlasers: Results from finite difference time domain simulations," Radio Sci. 31, 931–941 (1996).
18. S. Phang, A. Vukovic, S. Creagh, T. M. Benson, P. D. Sewell, and G. Gradoni, "Parity-Time Symmetric Coupled Microresonators with a Dispersive Gain/Loss," Opt. Express 23, 11493-11507 (2015).
19. F. Grossmann, V. A. Mandelshtam, H. S. Taylor, and J. S. Briggs, "Harmonic inversion of time signals and its applications," J. Chem. Phys. 107, 6756–6869 (1997).
20. S. G. Johnson, "Harminv," http://ab-initio.mit.edu/wiki/index.php/Harminv.
21. D. Jalas, A. Petrov, M. Eich, W. Freude, S. Fan, Z. Yu, R. Baets, M. Popović, A. Melloni, J. D. Joannopoulos, M. Vanwolleghem, C. R. Doerr, and H. Renner, "What is — and what is not — an optical isolator," Nat. Photonics 7, 579–582 (2013).